9th Plenary Workshop of the Muon g-2 Theory Initiative

University of Connecticut, USA, August 3 - 7, 2026

Status of the Experimental Inputs for HVP by SND

Kupich Andrey

BINP, Novosibirsk

on behalf of the SND collaboration

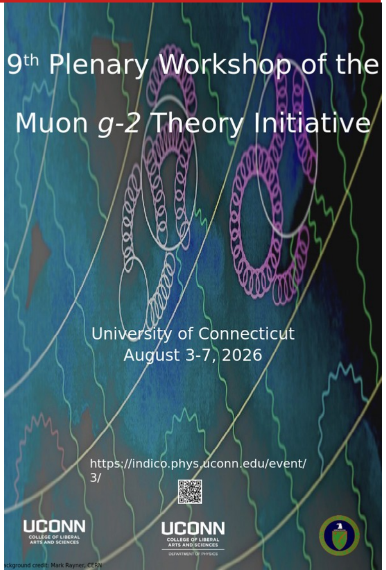

VEPP-2000 e^+e^- collider

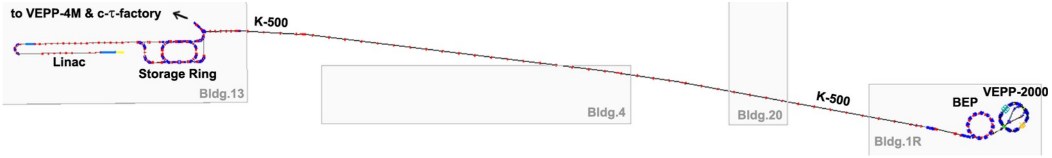

VEPP-2000 parameters:

- C.m. energy E=0.3-2.0 GeV
- Circumference – 24.4 m
- Number of bunches – 1×1
- Round beam optics
- Luminosity at E=1.8 GeV
  1×10^{32} cm^{-2} sec^{-1} (project)
  9×10^{31} cm^{-2} sec^{-1} (achieved)
- Two detectors: SND and CMD-3
- Energy measurements using Compton Backscattering

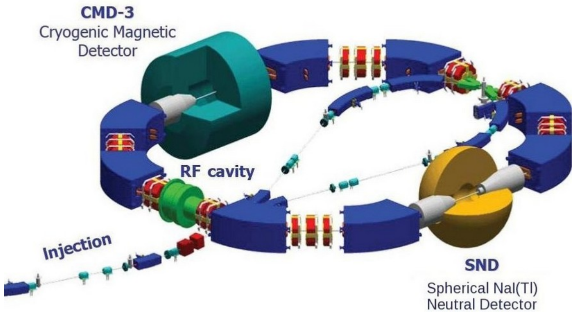

Beam energy measurements: CBS system

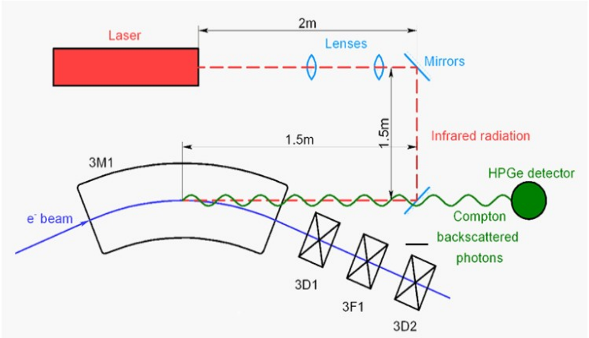

The systematic error of the beam energy determination is tested by comparison with a measurement using the resonance depolarization method:

$$\frac{\Delta E}{E} \leq 6\cdot10^{-5}$$

The high accuracy of collider beam energy determination is crucial for a lot of physical studies. For example, in order to measure the cross section of the process $e^+e^-\to\pi^+\pi^-$ with accuracy better than 1%.

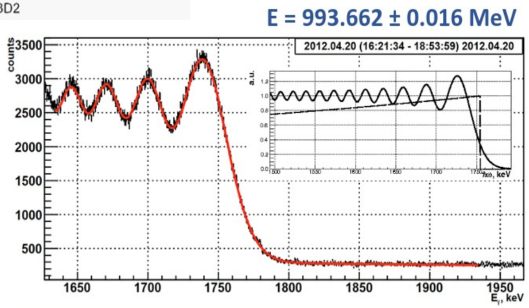

SND detector

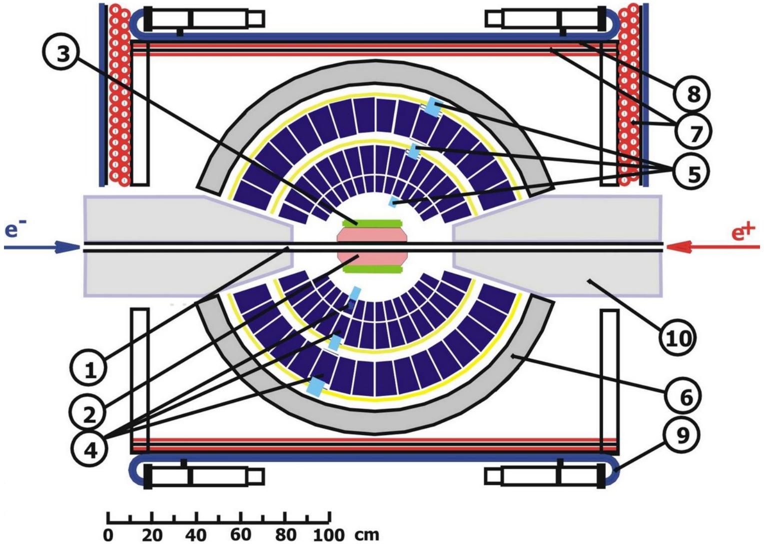

1 – beam pipe, 2 – tracking system, 3 – aerogel Cherenkov counter , 4 – NaI(Tl) crystals, 5 – phototriodes, 6 – iron muon absorber, 7–9 – muon detector, 10 – focusing solenoids.

Calorimeter

Thickness	$13.5\ X_0$
Acceptance	$0.95 \times 4\pi$
Energy resolution	$\frac{\sigma_E}{E} = \frac{0.042}{\sqrt[4]{E[GeV]}}$
Angular resolution	$\sigma_{\phi,\theta} = \frac{0.82^\circ}{\sqrt{E[GeV]}} \oplus 0.63^\circ$

Tracking system

Acceptance (9 layers)	$0.94 \times 4\pi$
Angular resolution	$\sigma_\phi = 0.55^\circ, \sigma_\theta = 1.2^\circ$
Vertex resolution	$\sigma_R = 0.12cm, \sigma_Z = 0.45cm$

The main physics task of SND is study of all possible processes of e^+e^- annihilation into hadrons below 2 GeV.

- ✓ The total hadronic cross section, which is calculated as a sum of exclusive cross sections.
- ✓ Dynamics of multihadron exclusive processes.
- ✓ Properties of vector mesons of the ρ, ω, φ families.
- ✓ Nucleon-antinucleon production near threshold.

Data collection

2010-2013 – 64 pb^{-1}
2013-2016 – stop
2017-2019 – 167 pb^{-1}
2020-2026 – 800 pb^{-1}

Total ~1 fb^{-1}

2024-2026 – Scan of the - region (150-500 MeV) with 3-fold increase in statistics

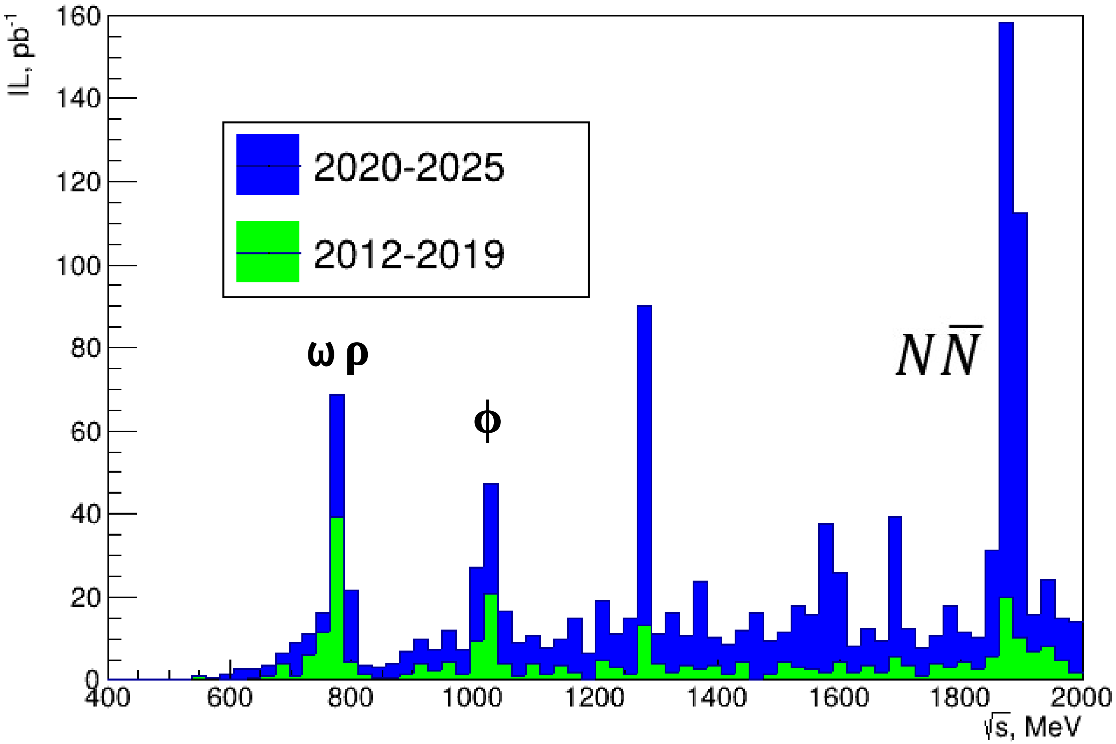

Motivation for the high precision measurements

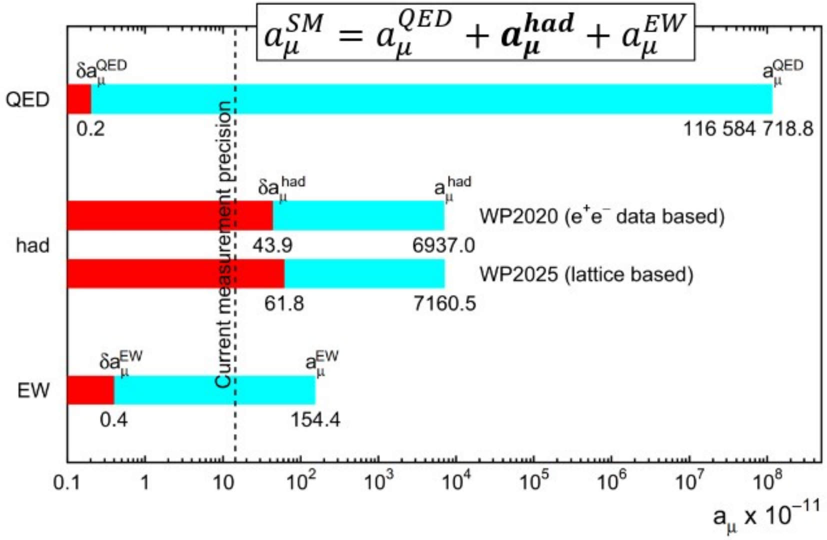

I. There is no tension: $a_\mu^{exp} - a_\mu^{SM} = 38(63) \cdot 10^{-11}$
II. The theoretical error is ~5 times greater than the experimental error
III. SM error is determined by the hadronic contribution a_μ^{had}
IV. The main contribution to a_μ^{had} is $a_\mu^{HVP\ LO}$
V. Finally, the main contribution to the magnitude and error of $a_\mu^{HVP\ LO}$ is given by $\pi^+\pi^-$ and $\pi^+\pi^-\pi^o$

$$a_\mu^{had} = \boldsymbol{a_\mu^{HVP\ LO}} + a_\mu^{HVP\ HO} + a_\mu^{HLbL}$$

had	HVP LO	HVP HO	HLbL
	$a_\mu[10^{-11}]$ (uncertainty)		
WP2020	6931 (40)	−85.9(0.7)	92 (18)
WP2025	7132 (61)	−87.2(1.3)	115.5 (9.9)

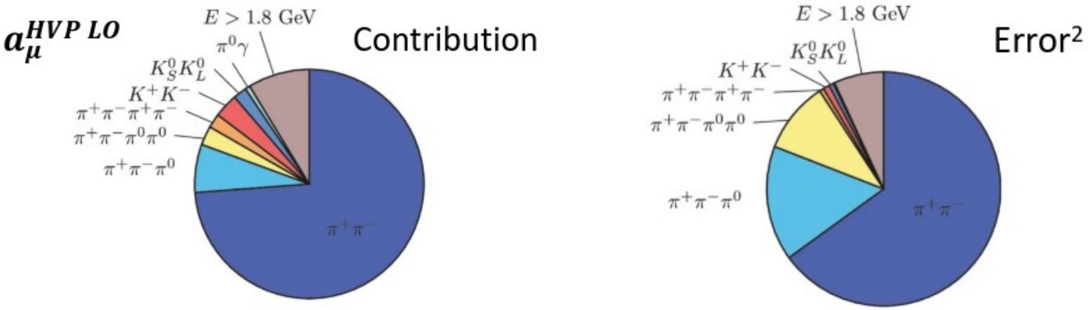

PR Vol. 1143, 2 (2025), PP 1-158

$e^+e^- \to \pi^+\pi^-$ for the $\sqrt{s}<1$ GeV

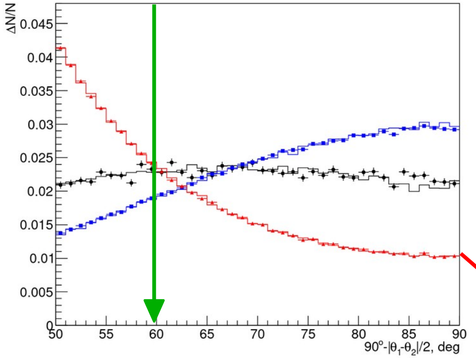

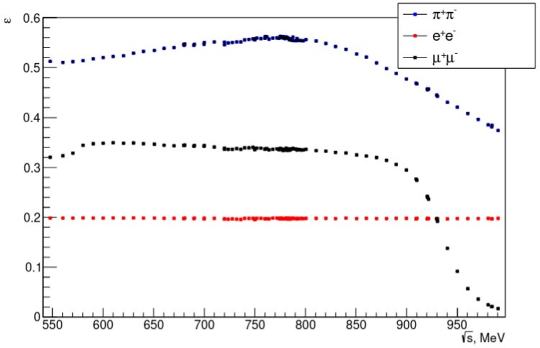

Selection criteria:

- Number of charge particles >=2
- Origin from e^+e^- collision:
  - $|r_i| < 1$ cm
  - $|z_i| < 8$ cm
- Collinearity:
  - $|\Delta\theta| < 14^\circ$
  - $|\Delta\varphi| < 6^\circ$
- Polar angle: $60^\circ < \theta_0 < 120^\circ$
- Particle energy deposition: $E_{1,2} > 40$ MeV
- Cosmic veto
- **Identification in calorimeter**

Background processes:

1. $e^+e^- \to \mu^+\mu^-$
2. $e^+e^- \to e^+e^-$
3. Cosmics
4. $e^+e^- \to e^+e^-e^+e^-$ (0.2-3.5%)
5. $e^+e^- \to \pi^+\pi^-\pi^0$ (0.01-0.6%)

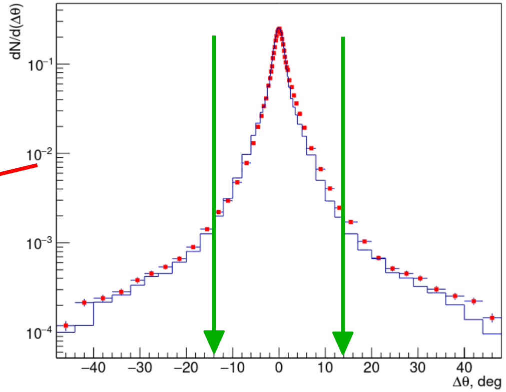

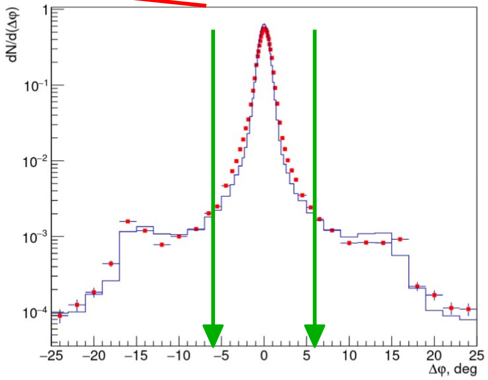

$e^+e^- \to \pi^+\pi^-$: selection without veto

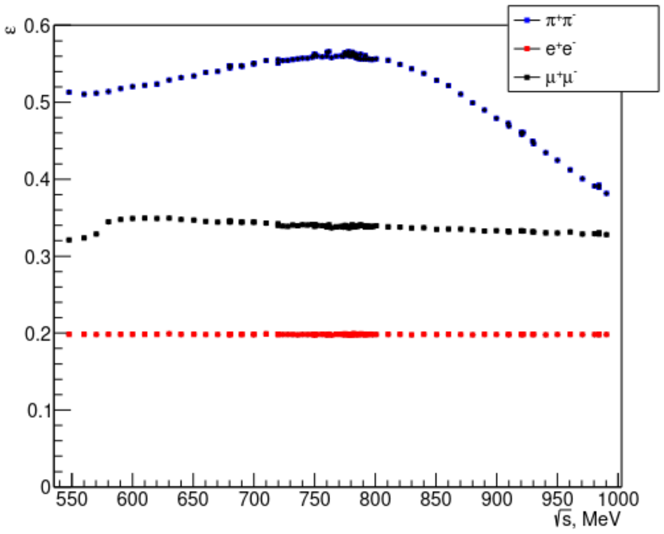

Without cosmic veto for √s>0.9 GeV

Number of CBE is derived from the vertex position fit

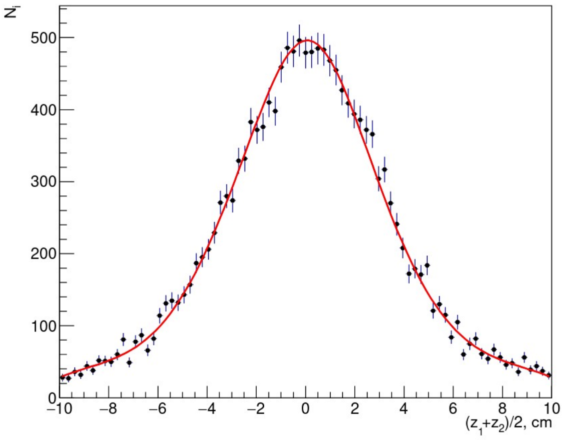

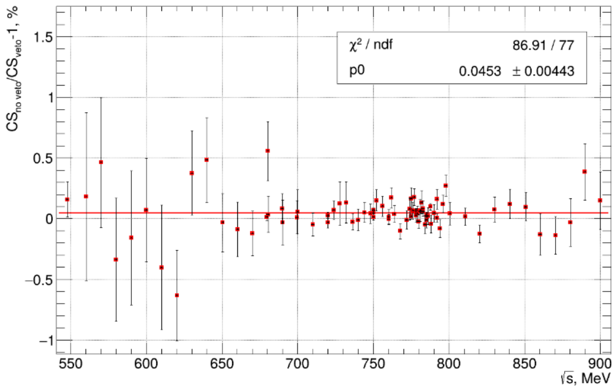

Both methods show similar results for √s<0.9 GeV

$e^+e^- \to \pi^+\pi^-$: parameters for the event ID

Different energy deposition profiles for **pions**, **electrons** and **muons**

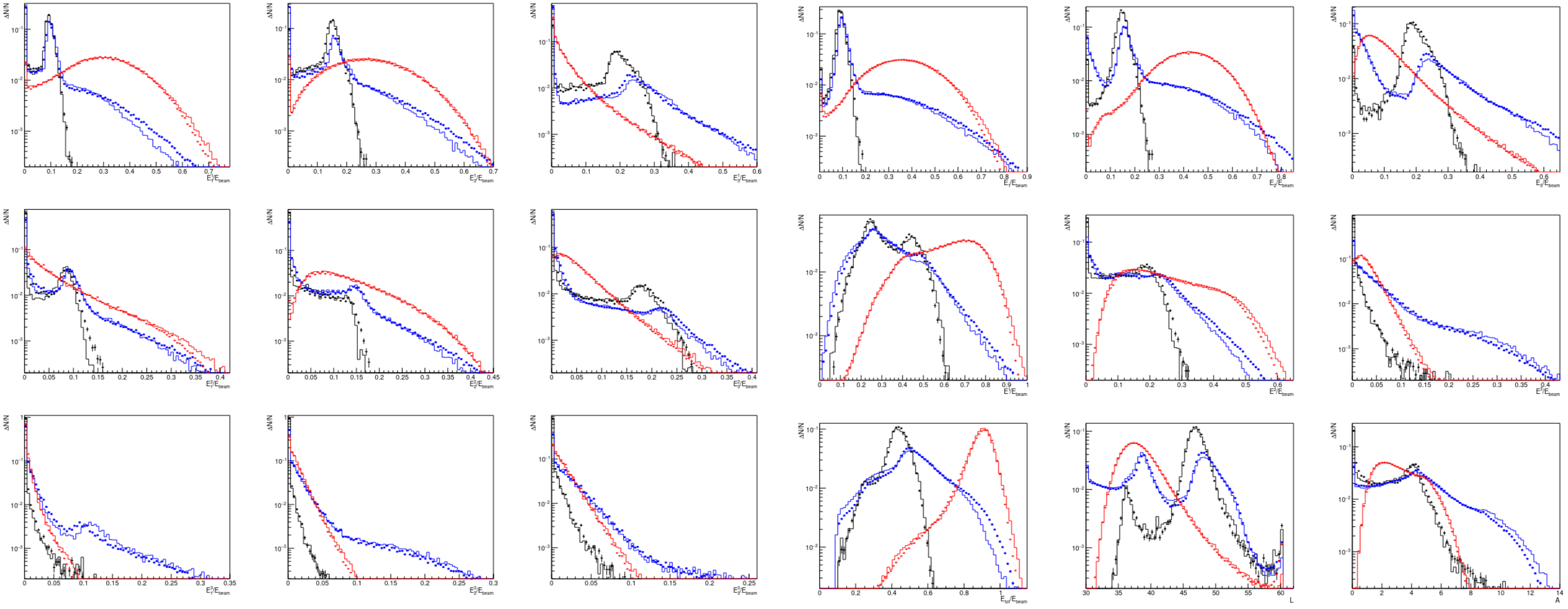

$e^+e^- \to \pi^+\pi^-$: output for ID algorithm

Machine learning method (**Gradient Boosted Decision Trees**) demonstrated the best separation performance, with total of **36** input parameters

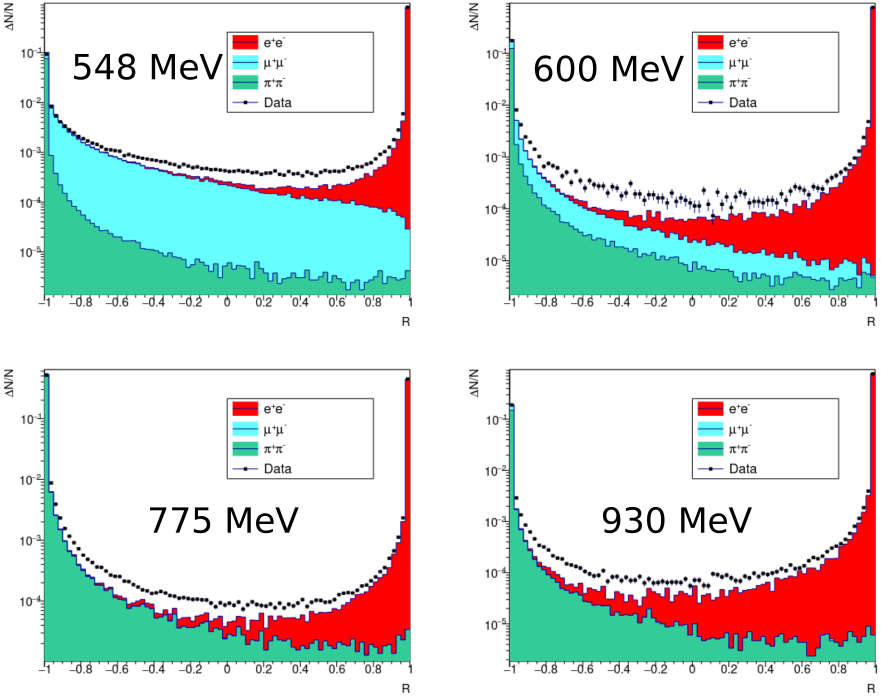

Similar **e/π** and **μ/π** separation algorithms are also constructed, but for individual particles, with **18** input parameters

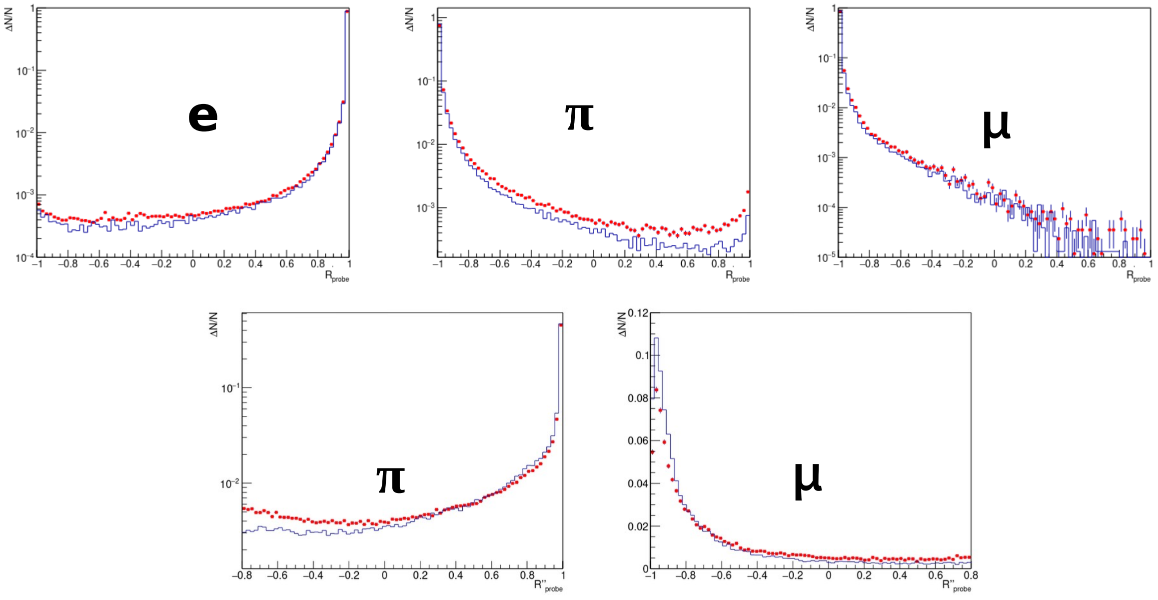

Used to create pure samples of events and pseudo-events

$e^+e^- \to \pi^+\pi^-$: major (+new) sources of syst. errors

Variation of E_{dep}>40 MeV correction

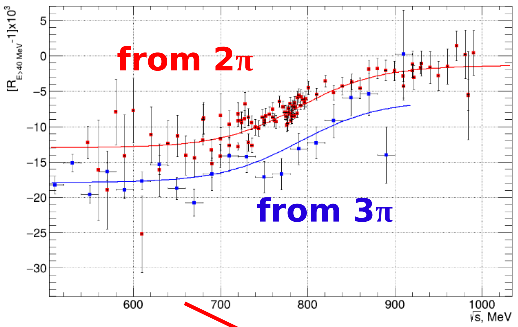

Variation of polar angle cut

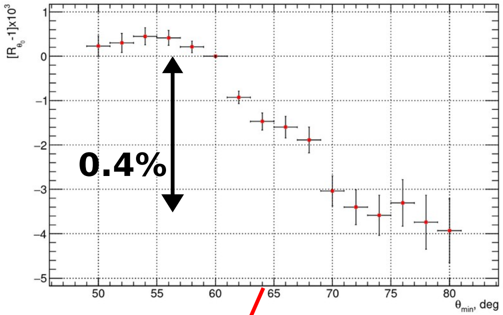

Uncertainty of the correction for e/π selection efficiency

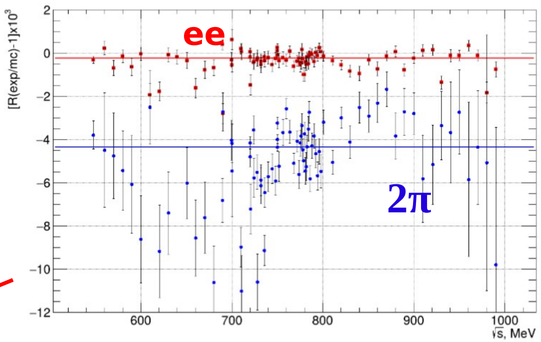

From muon background subtraction

$$\sigma_\mu = (\sigma_{\theta_0} \oplus \sigma_\Delta \oplus \sigma_{rad}) \times \frac{\varepsilon^1_{\mu\mu}\sigma_{\mu\mu}}{\varepsilon^1_{\pi\pi}\sigma_{\pi\pi}}$$

Variation of triggers

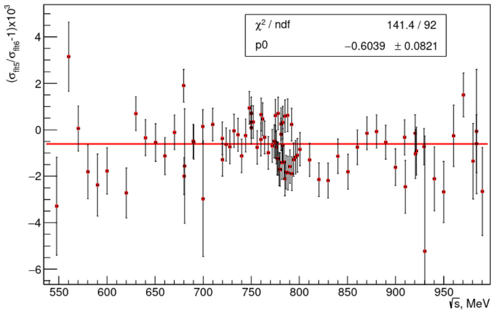

Error	$600 < \sqrt{s} < 900$ MeV, %	$\sqrt{s} \leq 600$ MeV and $\sqrt{s} \geq 900$ MeV, %
$\sigma_{e/\pi}$	0.05–0.1	0.1–0.3
σ_μ	0.03–0.1	0.1–0.3
σ_Δ	0.2	
σ_{θ_0}	0.4	
$\sigma_{E>40}$	0.5	
$\sigma_{nc>1}$	0.1	
σ_{rad}	0.1	
σ_{uncor}	0.1	
σ_{nucl}	0.1	
total	0.7	0.7–0.8

Correction for probability of pion loss in the vacuum chamber

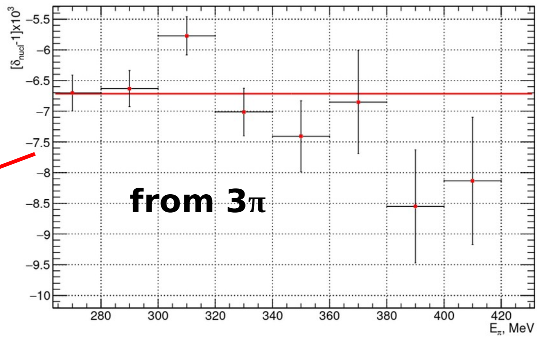

Current estimates of systematic error: **0.7-0.8%**.

$e^+e^- \to \pi^+\pi^-$: Fit of the data

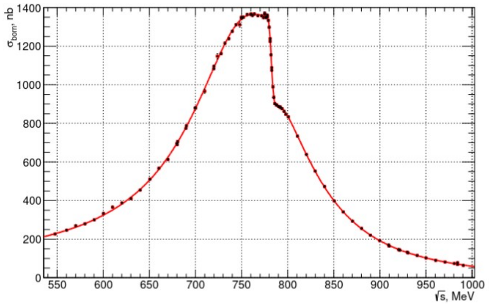

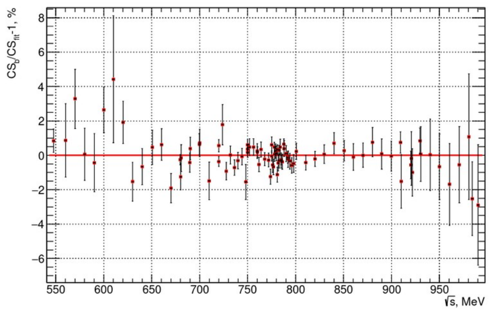

Current analysis is based on 2018 data (47 pb^{-1}), collected below 1 GeV. **BabaYaga-NLO** generator is implemented in MC. Process $e^+e^- \to e^+e^-$ is used for IL measurement, it's separated from other events with the machine learning methods. Efficiency corrections are based on study of experimental events. With radiative and beam energy spread corrections born cross section is calculated.

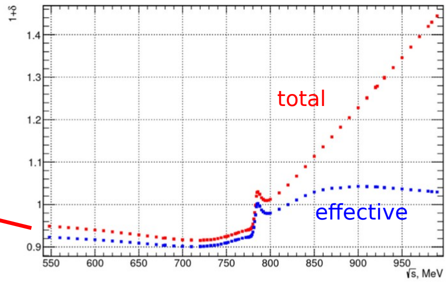

$$\sigma^0_{\pi\pi}(s_i) = \frac{\sigma_{\pi\pi}(s_i)}{1+\delta_{rad}(s_i)}$$

$$\sigma_{\pi^+\pi^-} = \frac{\pi\alpha^2}{3s}\beta^3_\pi\,|F_\pi(s)|^2$$

	n-r contr = 0	n-r contr ≠ 0
Γ_ω = const	BL	A1
Γ_ω ≠ const	A2	A3

$$F_\pi(s) = \frac{GS_\rho(s)\left(1+\frac{A_\omega s}{s-m^2_\omega+im_\omega\Gamma_\omega}\right)+\beta\cdot GS_{\rho'}(s)+\delta\cdot GS_{\rho''}(s)}{1+\beta+\delta}$$

Born cross section is fitted with VMD: **ρ(770)**, ρ(1450),ρ(1700) and **ω**

200 KeV Off from PDG

Parameter	Baseline model	A1
m_ρ, MeV	775.769 ± 0.143 ±0.084	775.809 ± 0.148 ±0.132
Γ_ρ, MeV	149.649 ± 0.26 ±0.112	149.579 ± 0.276 ±0.153
m_ω, MeV	782.443 ± 0.064 ±0.06	782.45 ± 0.064 ±0.061
Γ_ω, MeV	8.906 ± 0.137 ±0.061	8.909 ± 0.137 ±0.063
$B(\omega\to\pi^+\pi^-)\cdot B(\omega\to e^+e^-)$, 10^{-6}	1.212 ± 0.021 ±0.008	1.21 ± 0.021 ±0.01
$\lvert\beta\rvert$	0.746 ± 0.002 ±0.061	0.404 ± 0.013 ±0.107
$\lvert\delta\rvert$	0.726 ± 0.002 ±0.077	0.581 ± 0.077 ±0.525
$\phi_{\rho\omega}$, rad.	0.179 ± 0.013 ±0.003	0.174 ± 0.013 ±0.008
$\phi_{\rho\rho'}$, rad.	-1.07 ± 0.005 ±0.073	-0.515 ± 0.121 ±1.127
$\phi_{\rho\rho''}$, rad.	2.8 ± 0.007 ±0.058	3.835 ± 0.007 ±1.691
$\lvert c\rvert$	—	0.273 ± 0.014 ±0.442
arg(c), rad.	—	2.558 ± 0.124 ±2.56
χ^2/ndf	108/83	107.8/81

Parameter	A2	A3
m_ρ, MeV	775.759 ± 0.142 ±0.074	775.91 ± 0.154 ±0.143
Γ_ρ, MeV	149.666 ± 0.259 ±0.1	149.644 ± 0.304 ±0.062
m_ω, MeV	782.77 ± 0.065 ±0.06	782.786 ± 0.068 ±0.061
Γ_ω, MeV	8.975 ± 0.139 ±0.061	8.991 ± 0.143 ±0.065
$B(\omega\to\pi^+\pi^-)\cdot B(\omega\to e^+e^-)$, 10^{-6}	1.209 ± 0.021 ±0.009	1.202 ± 0.021 ±0.018
$\lvert\beta\rvert$	0.729 ± 0.002 ±0.018	0.26 ± 0.04 ±0.523
$\lvert\delta\rvert$	0.727 ± 0.002 ±0.043	0.071 ± 0.005 ±0.656
$\phi_{\rho\omega}$, rad.	0.251 ± 0.013 ±0.001	0.237 ± 0.014 ±0.022
$\phi_{\rho\rho'}$, rad.	-1.039 ± 0.006 ±0.068	-1.669 ± 0.044 ±0.731
$\phi_{\rho\rho''}$, rad.	2.836 ± 0.006 ±0.07	2.203 ± 0.078 ±0.882
$\lvert c\rvert$	—	0.148 ± 0.014 ±0.059
arg(c), rad.	—	-2.81 ± 0.165 ±1.169
χ^2/ndf	108/83	107.8/81

$e^+e^- \to \pi^+\pi^-$: Alternative model

N. N. Achasov and A. A. Kozhevnikov *Electromagnetic form factor of the pion in the field-theory-inspired approach* *Phys. Rev.* **D 85**, 019901 (2012)

$$\sigma_{pol} = \frac{\pi\alpha^2}{3s}\beta_\pi^3 \left|F_\pi^0(s)\right|^2 \left(1 + \frac{\alpha}{\pi}a(s)\right)$$

$$g_{\gamma V} = \sqrt{\frac{3\Gamma_{V\to e^+e^-} m_V^3}{4\pi\alpha^2}}, \quad V = \omega, \rho_1, \rho_2, \rho_3,$$

$$F_\pi^0(s) = \left(g_{\gamma\rho_1},\, g_{\gamma\rho_1},\, g_{\gamma\rho_2}\right) G^{-1} \begin{pmatrix} g_{\rho_1\pi\pi} \\ g_{\rho_2\pi\pi} \\ g_{\rho_3\pi\pi} \end{pmatrix} + g_{\gamma\omega}\Pi_{\rho_1\omega} \frac{G_{11}^{-1} g_{\rho_1\pi\pi} + G_{12}^{-1} g_{\rho_2\pi\pi} + G_{13}^{-1} g_{\rho_3\pi\pi}}{m_\omega^2 - s - i\sqrt{s}\Gamma_\omega(s)}$$

$$G_{ij} = \delta_{ij}(m_{\rho_i}^2 - s) - \Pi_{\rho_i\rho_j}(s), \quad i, j = 1, 2, 3$$

$$\Pi_{\rho_1\omega}(s) = \frac{s}{m_\omega^2}\Pi'_{\rho_1\omega} + i\sqrt{s}\left(\sqrt{\Gamma_{\omega\to\pi^0\gamma}(s)\Gamma_{\rho\to\pi^0\gamma}(s)} + \sqrt{\Gamma_{\omega\to\eta\gamma}(s)\Gamma_{\rho\to\eta\gamma}(s)}\right)$$

$e^+e^- \to \pi^+\pi^-$: Alternative model

Parameter	Original model	Modified model
m_ρ, MeV	$776.3 \pm0.15\pm0.06$	$777.09 \pm0.18\pm0.06$
$\Gamma^{phys}_{\rho\to\pi^+\pi^-}$, MeV	$150.\pm0.3\pm0.08$	$149.44\pm0.3\pm0.08$
$\Gamma^{phys}_{\rho\to e^+e^-}$, keV	$7.486 \pm 0.044\pm0.03$	$7.475 \pm 0.058\pm0.03$
m_ω, MeV	$782.44 \pm0.03\pm0.08$	$782.92 \pm0.06\pm0.08$
Γ_ω, MeV	$8.71 \pm0.13\pm0.08$	$8.96 \pm0.13\pm0.08$
$\Pi'_{\rho_1\omega}$, GeV^2	$2.878\pm0.05\pm0.013$	$2.917\pm0.05\pm0.013$
Z_{ρ_1}	0.928	0.929
k_{im}	—	$3.32\pm0.26\pm0.001$
χ^2/n.d.f.	198.8/84	117.4/83

$$\Gamma^{phys}_{\rho\to\pi^+\pi^-} = \frac{g^2_{\rho_1\pi\pi} m_{\rho_1} \beta^3_\pi(m^2_{\rho_1})}{48\pi Z_{\rho_1}}$$

$$\Gamma^{phys}_{\rho\to e^+e^-} = \frac{\Gamma_{\rho_1\to e^+e^-}}{Z_{\rho_1}}$$

$$Z_{\rho_1} = 1 + \left.\frac{d\mathrm{Re}(\Pi_{\rho_1\rho_1}(s))}{ds}\right|_{s=m^2_{\rho_1}}$$

Im($\Pi_{\rho\omega}$) is multiplied by k_{im}

$e^+e^- \to \pi^+\pi^-$: comparing with old data

Relative to the fit curve from current measurement

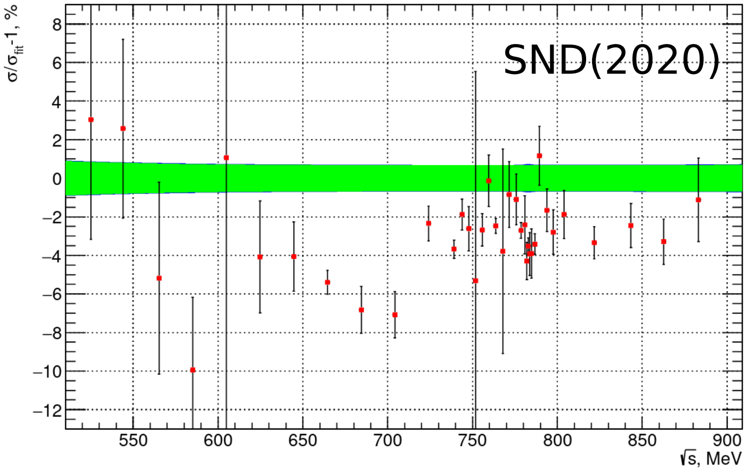

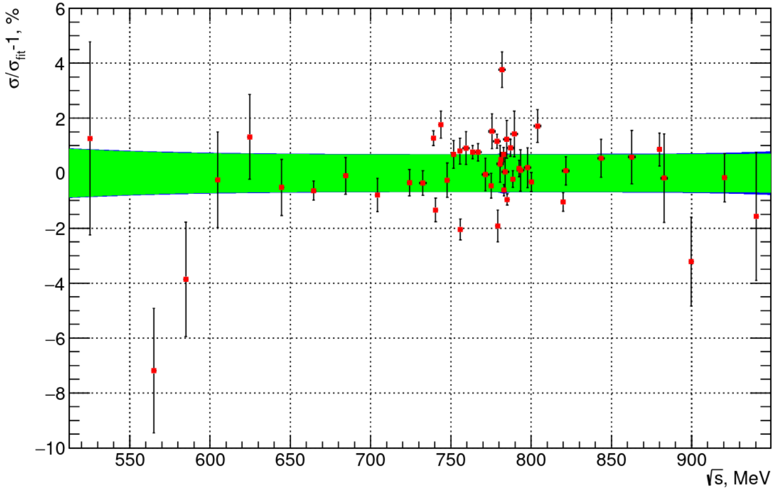

New measurement is 3% higher then previously published SND results
J. High Energ. Phys. 2021, 113 (2021)

After re-analysis the **2012-2013 SND** data (used in the last SND publication) is more consistent with new results. **Current explanation:** shortcomings of the old version of reconstruction resulted in unaccounted loss of the pion tracks.

$e^+e^- \to \pi^+\pi^-$: comparing with other experiments

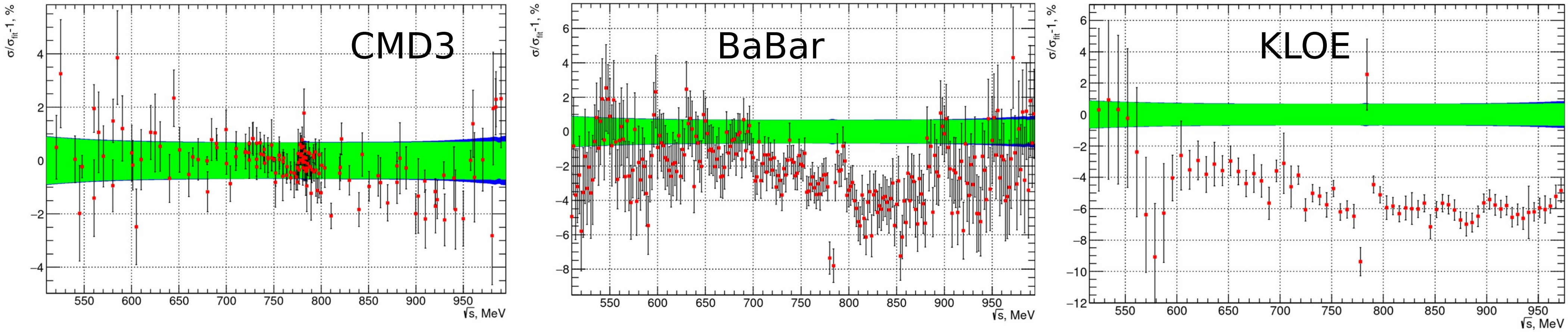

New SND result is consistent with **CMD3**

SND measurement is consistent with old **BaBar** results below ρ, and 3% higher above 0.78 GeV

Our measurement is 2-6% higher than combined **KLOE** result

Stat. errors for dots

green band - syst. uncertainty
blue one — total error

$e^+e^- \rightarrow \pi^+\pi^-$

Contribution to g-2

The value of the anomalous magnetic moment according to the results of this work, BABAR and CMD3 calculated in the interval of [548 – 990] Mev

Cover ≈ 80% of total $\pi^+\pi^-$ contribution

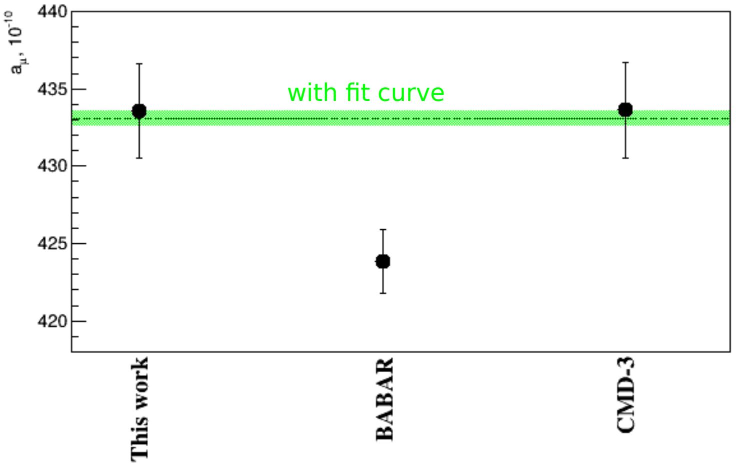

The contribution of the $e^+e^- \rightarrow \pi^+\pi^-$ to the anomalous magnetic moment of the muon in the leading order of perturbation theory is expressed through the dispersion relation:

$$a_\mu(\pi\pi, \sqrt{s_{max}} \leq \sqrt{s} \leq \sqrt{s_{min}}) = \left(\frac{\alpha m_\mu}{3\pi}\right)^2 \int_{s_{min}}^{s_{max}} \frac{R(s)K(s)}{s^2} ds,$$

$$R(s) = \sigma^{pol}_{\pi\pi} \times \frac{3s}{4\pi\alpha^2} \quad \sigma^{pol}_{\pi\pi}(s) = \sigma^0_{\pi\pi}(s) \times |1 - \Pi(s)|^2 \times (1 + \frac{\alpha}{\pi} a(s))$$

https://cmd.inp.nsk.su/ ignatov/vpl/

$e^+e^- \to \pi^+\pi^-\pi^0$ in the 0.61-1.1 GeV region

Selection criteria:

- Number of charge particles >=2
- Number of neutral particles >=2
- Origin from e^+e^- collision:
  - $|r_i| < 1$ cm
  - $|z_i| < 15$ cm
  - $|z_1 - z_2| < 5$ cm
- Kinematic reconstruction:
  - Finding a common vertex given the beam collision point for two charged particles
  - Kinematic reconstruction in hypothesis $e^+e^- \to \pi^+\pi^-\gamma\gamma$
  - If there are several photons in the event, then the combination with the smallest χ^2 is selected
  - $\chi^2 < 100$
- Additional conditions for different energy region
- **Identification by the invariant mass $M_{\gamma\gamma}$**

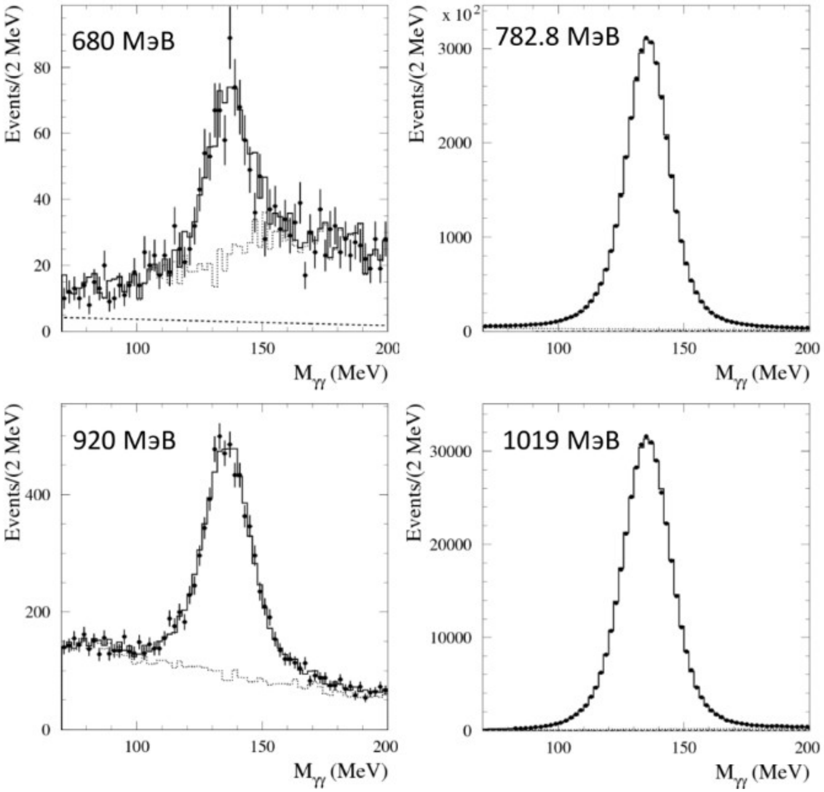

Background processes:

$\pi^+\pi^-(\gamma)$

$e^+e^-(\gamma\gamma)$

$\mu^+\mu^-(\gamma\gamma)$

$\eta\gamma$

$\pi^0\gamma$

$\pi^0 e^+e^-$

$\pi^0\pi^0\pi^+\pi^-$

$K^+K^-,\ K_S K_L$

$e^+e^- \to \pi^+\pi^-\pi^0$ in the 0.61-1.1 GeV region

Data from 2018, 102 points, luminosity 66 pb^{-1}

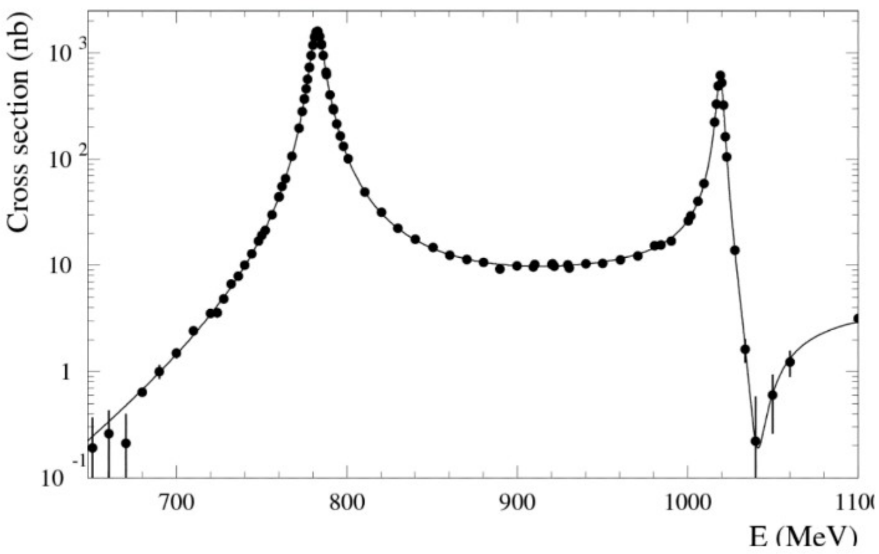

Parameter	Fitted value	PDG value
$\mathcal{B}(\omega \to e^+e^-)\mathcal{B}(\omega \to 3\pi) \times 10^5$	$6.648 \pm 0.022 \pm 0.058$	6.61 ± 0.16
m_ω, MeV	$782.703 \pm 0.011 \pm 0.047$	782.66 ± 0.13
Γ_ω, MeV	$8.598 \pm 0.023 \pm 0.004$	8.68 ± 0.13
$\mathcal{B}(\phi \to e^+e^-)\mathcal{B}(\phi \to 3\pi) \times 10^5$	$4.154^{+0.102}_{-0.066} \pm 0.066$	4.42 ± 0.11
m_ϕ, MeV	$1019.488 \pm 0.017 \pm 0.061$	1019.460 ± 0.016
Γ_ϕ, MeV	$4.265 \pm 0.033 \pm 0.014$	4.249 ± 0.013
φ_ϕ, deg	$156.8^{+6.5}_{-4.6} \pm 1.9$	163 ± 7
$\mathcal{B}(\rho \to 3\pi) \times 10^5$	$4.7 \pm 1.2 \pm 1.3$	9 ± 4
φ_ρ, deg	$-95.3 \pm 8.3 \pm 4.0$	-99 ± 17

Source of systematics	near ω	near ϕ	Between ω and ϕ
Luminosity	0.7	0.7	0.7
Events	0.2	0.6	0.8
Efficiency	0.5	0.8	1.0
Total	0.9	1.2	1.5

Fit model:

- VDM: $\omega(782) + \rho(770) + \phi(1020) + \omega(1420)$
- The phase $\omega(1420)$ relative to $\omega(782)$ is fixed at 180°
- To the statistical error in the number of $\pi^+\pi^-\pi^o$ events, an additional spread of about $\sim 0.6\%$ was added

$e^+e^- \rightarrow \pi^+\pi^-\pi^0$ in the 0.61-1.1 GeV region

SND in comparison with other experiments near ω

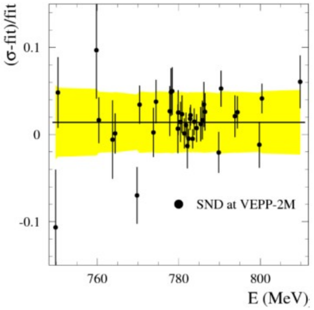

Our measurement is consistent with the BABAR and SND data on VEPP-2M, 4% (2σ) higher than the CMD-2 result and 8% (2σ) lower than the Belle-II result

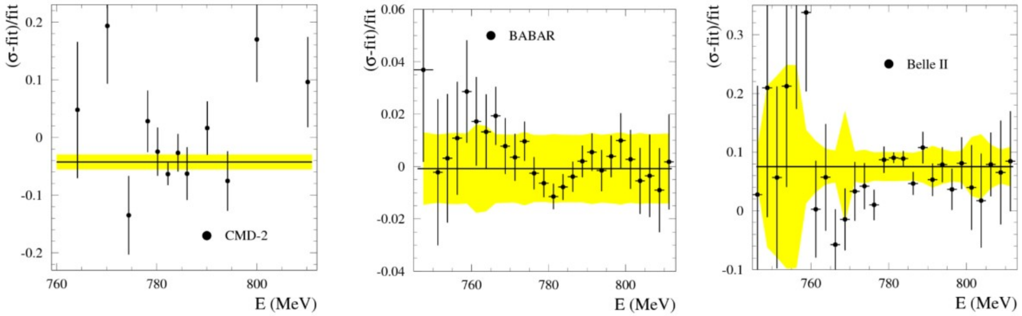

SND in comparison with other experiments near ϕ

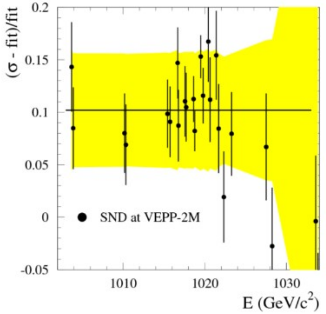

Our measurement is consistent with the BABAR and CMD-2 data, 10% (2 σ) lower than the SND results on VEPP-2M and 7% (2 σ) lower than the Belle-II result

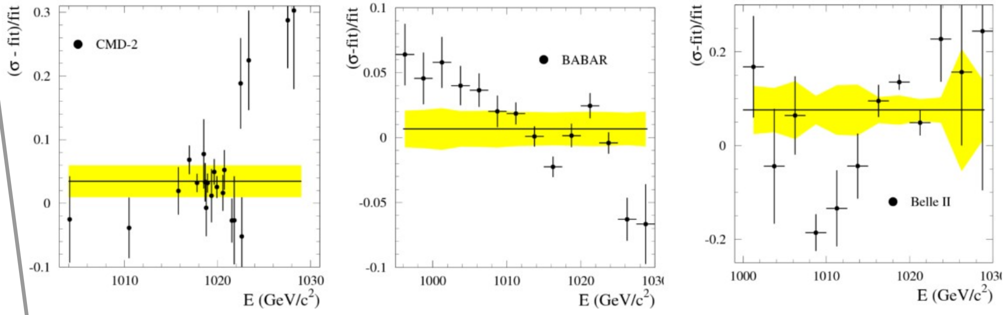

$e^+e^- \to \pi^+\pi^-\pi^0$ in the 0.61-1.1 GeV region

To calculate $a_\mu^{3\pi}$ below 1.1 GeV, an approximating function was used. The statistical error was determined using the toy MC. The systematic error in $a_\mu^{3\pi}$ was determined by shifting the measured cross section up or down by the systematic error.

The contribution of the SND to $a_\mu^{3\pi}$ above 1.1 GeV was calculated using data from the paper M.N. Achasov *et al.*, Phys. Atom. Nucl. **87**, 747(2024)

$$a_\mu^{3\pi} = \frac{\alpha^2}{3\pi^2}\int_{m_\pi^2}^{\infty}\frac{K(s)}{s}\frac{\sigma(s)|1-\Pi(s)|^2}{4\pi\alpha^2/s}ds$$

E, GeV	$a_\mu^{3\pi}\times 10^{10}$
0.61–1.10 (SND)	$42.96 \pm 0.06 \pm 0.45$
1.10–1.975 (SND)	$2.99 \pm 0.02 \pm 0.08$
0.61–1.975 (SND)	$45.95 \pm 0.06 \pm 0.46$
0.62–1.10 (BABAR)	$42.91 \pm 0.14 \pm 0.55 \pm 0.09$
1.10–2.00 (BABAR)	$2.95 \pm 0.03 \pm 0.16$
$<$ 2.00 (BABAR)	$45.86 \pm 0.14 \pm 0.58$
0.62–1.80 (Belle II)	$48.91 \pm 0.23 \pm 1.07$
$<$ 1.8 before 2021 *	$46.2 \pm 0.6 \pm 0.6$

* M. Hoferichter, B. L. Hoid and B. Kubis, JHEP 2019, 137 (2019)

The SND result is in agreement with the BABAR and $a_\mu^{3\pi}$ result calculated using data up to 2021, but is 2.5σ lower than the Belle II result

$e^+e^- \to \pi^+\pi^-\pi^0$ in the 1.06-2.0 GeV region

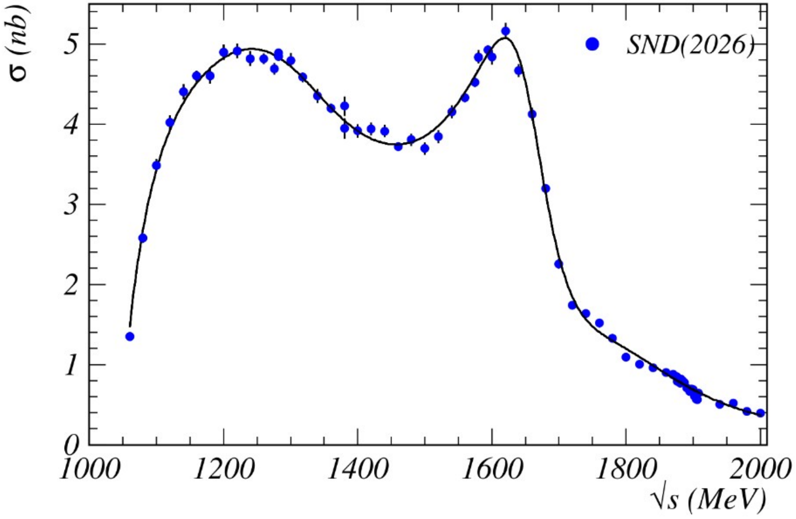

$$\frac{d\sigma}{d\Gamma} = \left|\alpha A_{\rho\pi} + \beta A_{\rho'\pi} + \gamma A_{\omega\pi}\right|^2$$

parameters	SND (previous)	this work
M(ω′) (MeV)	1350 ± 43	1215 ± 26
Γ (ω′) (MeV)	590 ± 90	480 ±33
σ (ω′ →ρπ) (nb)	4.17 ± 0. 73	1.35 ± 0.09
σ (ω′ →ρ′π) (nb)	$0.053^{+0.021}_{-0.015}$	0.72 ± 0.16
M(ω′′) (MeV)	1643 ± 6	1648 ± 5
Γ (ω′′) (MeV)	148 ± 13	173 ± 10
σ (ω′′→ρπ) (nb)	$0.046^{+0.042}_{-0.028}$	0.023 ± 0.012
σ (ω′′→ρ′π) (nb)	1.65 ± 0.16	1.54 ± 0.18
$M(\omega_x)$ (MeV)		1782 ± 20
$\Gamma(\omega_x)$ (MeV)		200 ± 10
σ (ω′′→ρπ) (nb)		0.36 ± 0.10
σ (ω′′→ρ′π) (nb)		0.11 ± 0.06

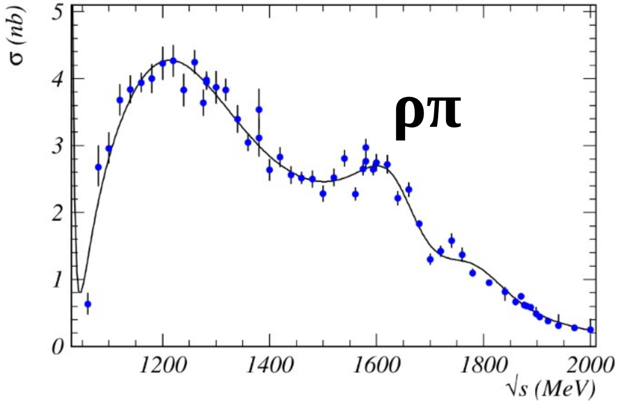

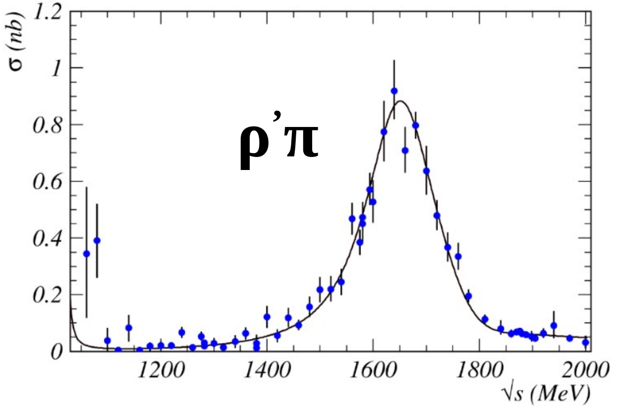

Background processes:

- $e^+e^- \to \pi^+\pi^-\pi^0\pi^0$
- $e^+e^- \to \pi^+\pi^-\gamma$
- $e^+e^- \to K_S K_L$
- $e^+e^- \to K^+K^-\pi^0$
- $e^+e^- \to \mu^+\mu^-\gamma$

Application of the simple quark model

$$|\omega\rangle = \cos\frac{\alpha}{2}\,|\omega_0\rangle - \sin\frac{\alpha}{2}e^{i\varphi}\,|\rho_0\rangle\,, \quad |\rho\rangle = \cos\frac{\alpha}{2}\,|\rho_0\rangle + \sin\frac{\alpha}{2}e^{-i\varphi}\,|\omega_0\rangle\,, \quad |\omega_0\rangle = \frac{|u\bar{u}\rangle + |d\bar{d}\rangle}{\sqrt{2}}, \quad |\rho_0\rangle = \frac{|u\bar{u}\rangle - |d\bar{d}\rangle}{\sqrt{2}}$$

$$\sqrt{\frac{\Gamma_{\omega\to\pi^+\pi^-}}{\Gamma_{\rho\to\pi^+\pi^-}}} = \tan\frac{\alpha}{2} = 0.03166 \longrightarrow \Gamma_{\rho\to\pi^+\pi^-\pi^0} = \Gamma_{\omega\to\pi^+\pi^-\pi^0}\cdot\tan^2\frac{\alpha}{2} \longrightarrow B(\rho\to\pi^+\pi^-\pi^0) = 3.6\cdot10^{-5}$$

$<1\sigma$

SND: $B(\rho\to\pi^+\pi^-\pi^0) = (4.7\pm1.8)\cdot10^{-5}$

From $A_{V\gamma}$ transition amplitude:

$$\frac{\Gamma_{\rho\to e^+e^-}}{\Gamma_{\omega\to e^+e^-}} = \frac{9+6\cdot\cos\varphi\cdot\tan\frac{\alpha}{2}+\tan^2\frac{\alpha}{2}}{1-6\cdot\cos\varphi\cdot\tan\frac{\alpha}{2}+9\cdot\tan^2\frac{\alpha}{2}}\cdot\left(\frac{m_\omega}{m_\rho}\right)^3 \longrightarrow 11.46$$

$\approx1\sigma$ $\approx2\sigma$

SND: 11.66 ± 0.18

PDG: 10.81 ± 0.34

Summary

- The most precise measurement of the $e+e- \to \pi^+\pi^-\pi^0$ process cross section at energies below 1.1 GeV has been achieved [arXiv:2603.01635]
- The systematic error in measuring the cross section near the ω and φ resonance maxima is 0.9% and 1.2%, respectively
- The SND data are consistent with the BABAR measurements and are approximately 7-8% (2σ) lower than the Belle II data
- The most precise measurements of the $B(\phi \to e+e-)B(\phi \to \pi^+\pi^-\pi^0)$, m_ω and Γ_ω parameters have been made within VDM framework
- Study of the $e+e- \to \pi^+\pi^-\pi^0$ process at energies above 1.1 GeV showed that **ω**(1420) and **ω**(1650) decay predominantly via ρπ and ρ'π mechanisms, respectively.
- The total cross section of the $e+e- \to \pi^+\pi^-$ process was measured in the $\sqrt{s} = 548 - 990$ MeV energy range with a systematic error of 0.7-0.8% at $\sqrt{s} < 600$ and $\sqrt{s} > 900$ MeV and 0.7% at $600 < \sqrt{s} < 900$ MeV
- The results are consistent with the CMD-3 measurement, and there is a difference with BABAR (KLOE) data at the 2σ ($>5\sigma$) level
- Contribution of the $e+e- \to \pi^+\pi^-$ process to the anomalous magnetic moment of the muon is $a_\mu = (433.59 \pm 0.44 \pm 2.9) \cdot 10^{-10}$ in the $548 < \sqrt{s} < 990$ MeV energy range
- Our a_μ for the $316 < \sqrt{s} < 975$ MeV (calculated with a fit curve) is 4.2±1% greater than KLOE result
- Phase for the ρ-ω mixing exceeds theoretical predictions
- Simple quark model hints at higher $e+e- \to \pi^+\pi^-$ cross section
- Publication is close to the completion (fall of 2026)

Final slide

Thank you for attention!

θ_0 cut variations for every energy point

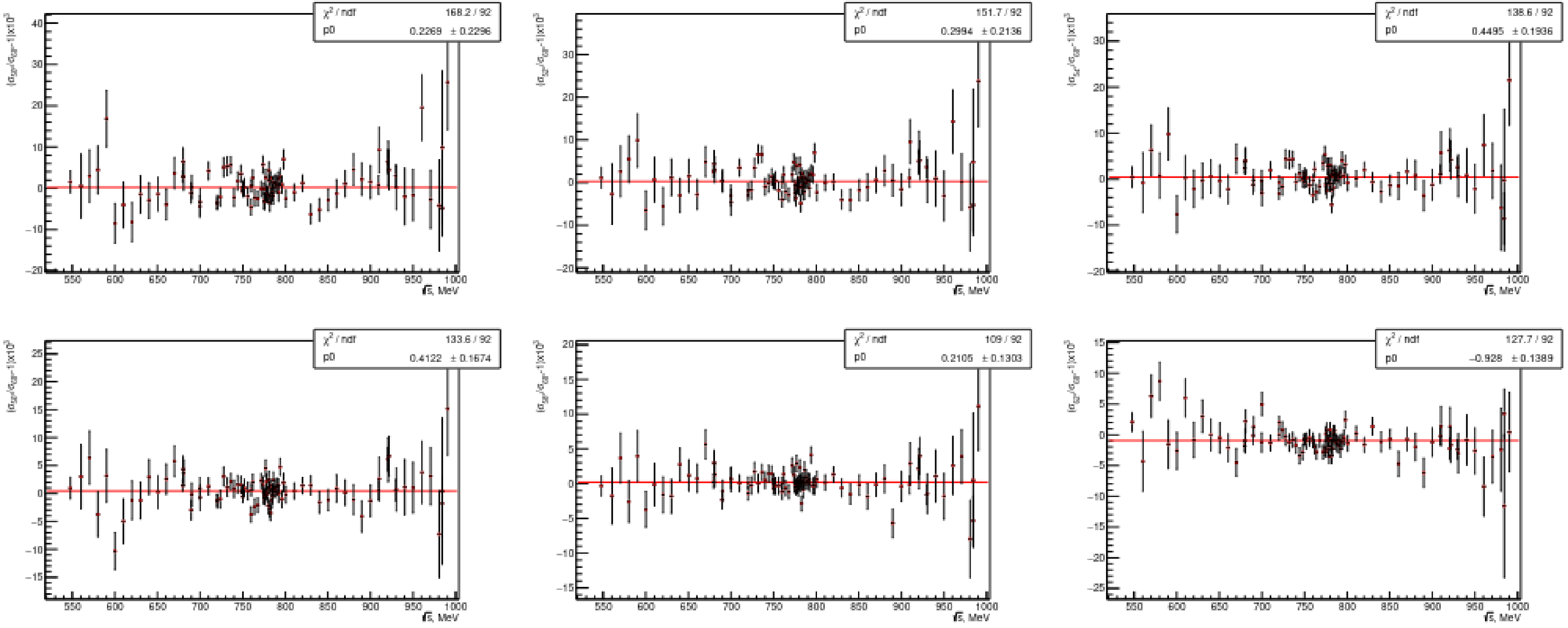

θ_0 cut variations for every energy point

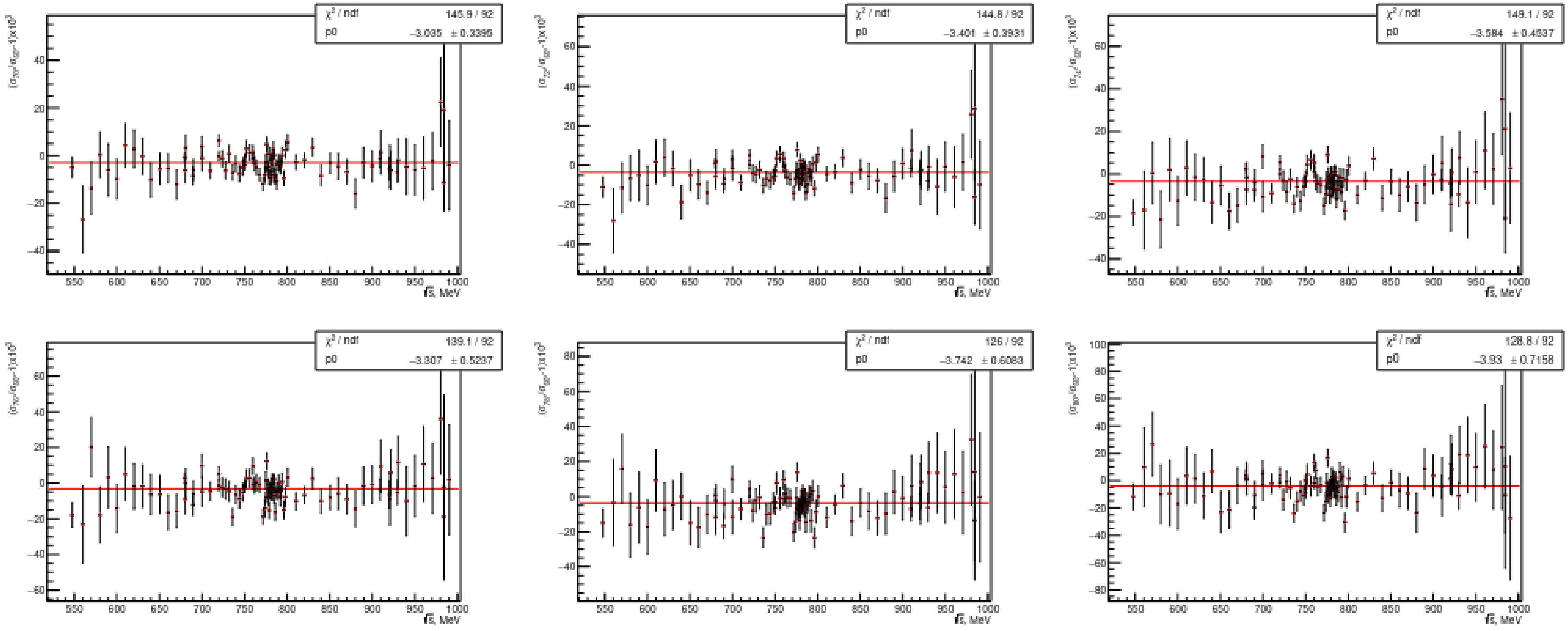

Collinearity distributions and corrections

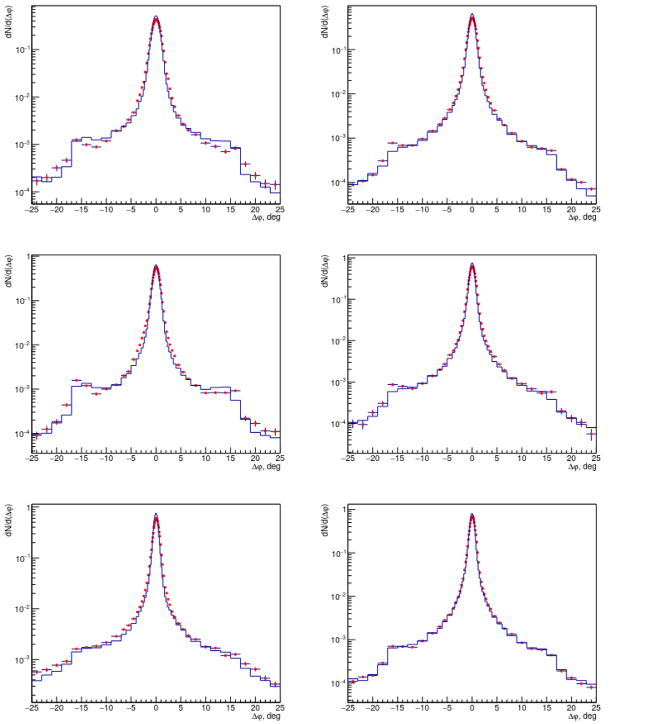

Figure 14. Distributions by $\Delta\phi$ for simulation events (histogram) and experiment (points with errors), left graphs - for events $e^+e^- \to \pi^+\pi^-$, right - $e^+e^- \to e^+e^-$ in the region of low (upper graphs) and high energies (lower), as well as the peak $\rho(770)$ (central)

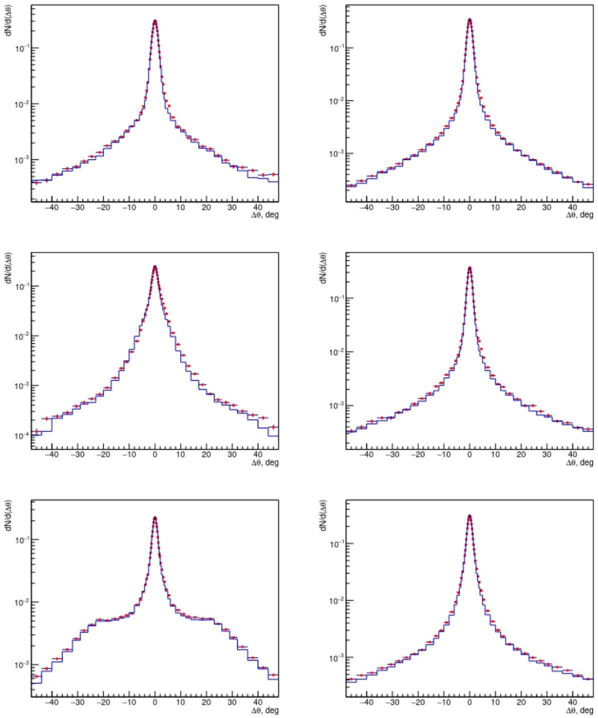

Figure 15. Distributions of $\Delta\theta$ for simulation events (histogram) and experiment (error bars). The left graphs are for $e^+e^- \to \pi^+\pi^-$ events, the right graphs are for $e^+e^- \to e^+e^-$ events in the low-energy (upper graphs) and high-energy (lower graphs), as well as the $\rho(770)$ peak (central)

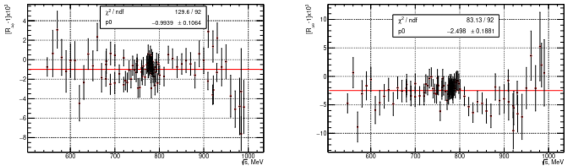

Figure 16. Corrections $R(\Delta\phi)$ (left graph) and $R(\Delta\theta)$ (right) depending on energy, for events $e^+e^- \to \pi^+\pi^-$. Line — averaging results.

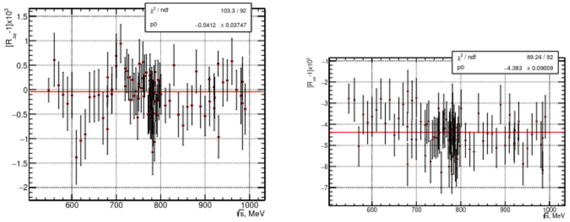

Figure 17. Corrections $R(\Delta\phi)$ (left graph) and $R(\Delta\theta)$ (right) depending on energy, for events $e^+e^- \to e^+e^-$. Line — averaging results.

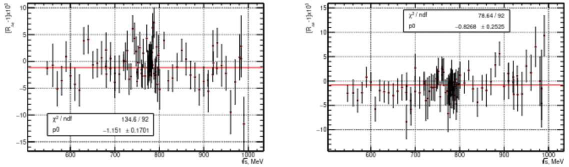

Figure 18. $R(\Delta\phi)$ (left graph) and $R(\Delta\theta)$ (right) corrections as functions of energy, for events $e^+e^- \to \mu^+\mu^-$.

Correction for the cosmic veto efficiency

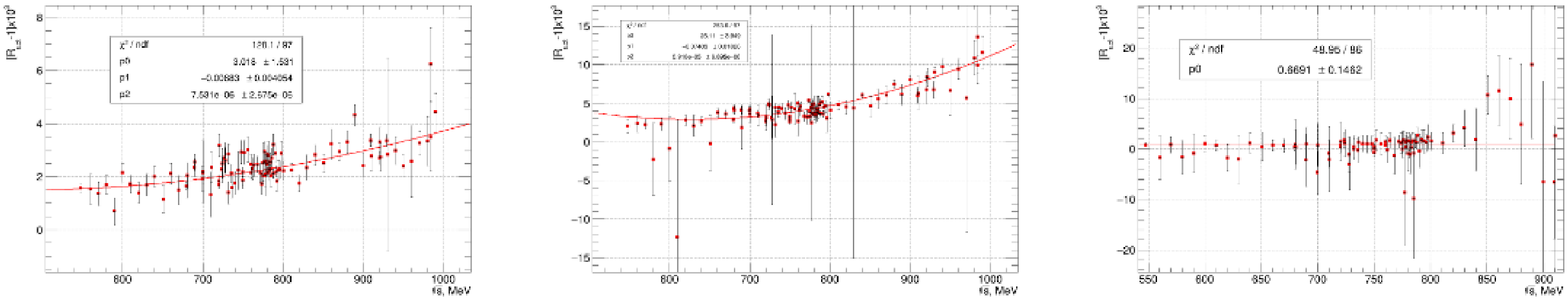

Figure 23. Efficiency corrections for the $veto = 0$ cut for the $e^+e^- \to e^+e^-$ (left graph), $e^+e^- \to \pi^+\pi^-$ (central) and $e^+e^- \to \mu^+\mu^-$ (right) events.